Distinct Structures and Environments for the Three Hemes of the Cytochrome bc_1 Complex from *Rhodospirillum rubrum*. A Resonance Raman Study Using B-Band Excitations

Carole Le Moigne,[‡] Barbara Schoepp,[§,||] Samya Othman,[‡,⊥] André Verméglio,[§] and Alain Desbois*[,‡]

Département de Biologie Cellulaire et Moléculaire, Section de Biophysique des Protéines et des Membranes, CEA et CNRS URA 2096, CEA/Saclay, F-91191 Gif-sur-Yvette Cedex, France, and Département de Physiologie Végétale et Ecosystèmes, Centre d'Etudes Nucléaires de Cadarache, F-13108 Saint-Paul-lez-Durance, France

Received March 10, 1998; Revised Manuscript Received October 28, 1998

ABSTRACT: The B-band excited resonance Raman (RR) spectra (100−1700 cm^{-1}) of the bacterial cytochrome bc_1 complex purified from *Rhodospirillum rubrum* are reported. Four redox states, i.e., the persulfate-oxidized, "as prepared", and ascorbate- and dithionite-reduced states of the complex, were investigated with the laser excitations at 406.7, 413.1, and 441.6 nm. Following the different absorption properties of the b- and c-type hemes and the different resonance enhancements of the vibrational modes of oxidized and reduced hemes, RR contributions from the b- and c-type hemes were characterized. For the ν_2, ν_{10}, and ν_8 porphyrin vibrational modes, individual contributions of hemes c_1, b_H, and b_L were determined. The data show that the macrocycle conformation of the three hemes of the cytochrome bc_1 complex is different. In particular, the frequencies assigned to ferrous heme b_L (1580, 1610, and 352 cm^{-1}, respectively) reveal that its porphyrin is more strongly distorted than that of ferrous heme b_H (1584, 1614, and 344 cm^{-1}, respectively). The frequencies of the ν_{11} modes (1543, 1536, and 1526 cm^{-1} for ferrous heme c_1, heme b_H, and heme b_L, respectively) confirm that the axial histidylimidazole ligands of heme b_L have a marked anionic character. Strong differences in the peripheral interactions of the three hemes with the proteins were also detected through the frequency differences of the ν_5, ν_{13}, ν_{14}, and ν_{42} modes. Considering that hemes b_H and b_L are inserted into a four-helice bundle, the RR data are interpreted in the frame of a strong protein constraint on heme b_L.

Oligomeric electron-transfer enzymes containing a monoheme c-type cytochrome[1] (cyt), a diheme cyt b, and a 2Fe-2S Rieske center are found in bacteria, chloroplasts, and mitochondria, and share many functional and structural properties (*1*−*7*). These membrane-bound proteins, named cyt bc_1 or cyt b_6f complexes, are involved in respiration in eukaryotic cells or participate in respiration, photosynthesis, denitrification and/or nitrogen fixation in bacteria (*1*−*3*). More precisely, these bc-type complexes catalyze the two-electron oxidation of a quinol (ubiquinol or plastoquinol) carrier and the one-electron reduction of a c-type cyt and link this electron transfer to the formation of a proton gradient across the membrane by a protonmotive Q cycle (*8, 9*). This gradient provides an energy source for ATP synthesis.

Several bacterial and mitochondrial cyt bc_1 complexes have been isolated, purified, and characterized (*3, 4*). The mitochondrial complexes contain between 7 and 11 protein subunits, whereas the bacterial complexes are simpler in terms of protein organization with 3−4 subunits (*4, 10*−*12*). Among the bacterial species, the bc_1 complex from *Rhodospirillum rubrum* has the minimal oligomeric structure with the diheme cyt b, cyt c_1, and Rieske protein and is able to accomplish the above-mentioned redox and proton translocation reactions. The additional subunit(s) observed in some bacterial and in all the mitochondrial complexes lack prosthetic groups and is (are) not essential to these reactions (*1, 7*). The redox potentials of the Rieske protein and of cyt c_1 are highly positive (E_m = 265−300 mV and 190−290 mV, respectively) (*1*). The cyt b subunit contains two inequivalent hemes with a high-potential heme b (b_H) and a low-potential heme b (b_L). Large dispersions in the E_m values of heme b_H (−30 to 100 mV) and heme b_L (−90 to −30 mV) are observed for the bacterial as well as for the mitochondrial complexes (*1, 4, 10*). Therefore, the simplest organization of the *R. rubrum* bc_1 complex constitutes a good model for structure studies in relation to the electron-transfer pathway for the different oligomeric bc_1 complexes.

The structure of the bc_1 complexes was investigated previously by both biochemical and spectroscopic methods. Cyt c_1 is held to the complex by a hydrophobic helix at the

* To whom correspondence should be addressed. Fax: 33 01 69 08 43 89. E-mail: desbois@dsvidf.cea.fr.

‡ CEA Saclay.

§ Centres d'Etudes Nucléaires de Cadarache.

|| Present address: Laboratoire de Bioénergétique et Ingénierie des Protéines, UPR CNRS 9036, 31 chemin Joseph Aiguier, F-13402 Marseille Cedex 20, France.

⊥ Present address: Laboratoire de Chimie et Biochimie Pharmacologiques et Toxicologiques, URA CNRS 400, Université Paris 5, 45 rue des Saints-Pères, F-75270 Paris Cedex 06, France.

[1] Abbreviations: cyt, cytochrome; RR, resonance Raman; FePP, iron protoporphyrin IX; ImH, imidazole; Im^-, imidazolate; BWHH, bandwidth at half-height; Vn, vinyl.

10.1021/bi9805487 CCC: $18.00
Published on Web 01/02/1999

C-terminus, and the heme domain is largely outside of the electropositive surface of the membrane (*7*). The side chains of His and Met residues provide the heme ligands of cyt c_1 (*3, 7*). The amino acid sequences of the cyt b subunit of cyt bc_1 and b_6f complexes have strong identities, substantiating models of common molecular organization in sequential transmembrane helices (*7, 13*−*16*). An eight-helix model is now widely accepted (*7, 10*). Investigations using electron paramagnetic resonance spectroscopy have located heme b_L near the P side of the membrane and heme b_H more central in the membrane (*17*). The recent crystallographic investigation of the cyt bc_1 complex from beef heart mitochondria has confirmed the previous model structures and the relative arrangements of the metal centers and the heme ligands (*12*). Among the four highly conserved His residues of the cyt b subunit (*3, 7*), H83 and H182 are identified as the heme b_L ligands, whereas H97 and H196 are the heme b_H ligands (*12*). Unfortunately, the 2.9-Å resolution of the most recent structure is not sufficient to give a detailed picture of the heme structures and heme/protein environments (*12*). Resonance Raman spectroscopy (RR) is however a powerful technique to obtain such structural data (*18, 19*). This vibrational method has been applied to the study of cyt bc_1 complexes from mitochondrial (*20*) and bacterial (*21, 22*) sources. In these studies, mainly the high-frequency regions of RR spectra excited in the Q-band (or $\alpha-\beta$) region have been investigated. However, the vibrational data extracted from B-band (or Soret)-excited RR spectra are more informative than, and distinct from, those obtained by Q-band excitations (*18*). Although the high-frequency regions of the Soret-excited spectra contain bands essentially corresponding to in-plane stretching modes of the tetrapyrrole macrocycle, the low- and mid-frequency regions involve modes associated with in-plane and out-of-plane deformations of the porphyrin or its peripheral groups and with the stretch or the deformation of the iron atom with its axial ligand(s) (*18, 23, 24*). The modes observed in all these regions are thus excellent probes for the characterization of the heme structures and heme/protein interactions (*25, 26*). Moreover, the B-band excitations of the RR spectra allow the study of ferriheme complexes and require smaller protein concentrations than the Q-band excitations. The present investigation reports the low-, mid-, and high-frequency RR spectra of the *R. rubrum* cyt bc_1 complex, excited at 406.7, 413.1, and 441.6 nm. Comparisons with Soret-excited RR spectra of monoheme proteins and model systems were made to interpret these spectra.

MATERIALS AND METHODS

Protein Preparations. The cyt bc_1 complex was prepared from *R. rubrum* (strain G9) and purified according to the method of Andrews et al. (*27*) with the following modification. The DEAE-Sepharose CL-6B column step was replaced by a second DEAE-BioGel A column step. The purified cyt bc_1 preparations (80−120 μM) were in 35 mM Mops buffer (pH 7.4) containing 1 mM $MgSO_4$, 100 mM NaCl, and 0.1 mg/mL dodecylmaltoside. They were checked by electrophoresis. The absorption spectra of the oxidized and ascorbate- and dithionite-reduced forms of the purified bc_1 complex were found very similar to those previously published for bacterial bc_1 complexes (Table 1 and refs *28, 29*).

Table 1: Absorption Maxima (nm) of the *R. rubrum* Cytochrome bc_1 Complex

cyt bc_1	Soret	β	α
oxidized	414	530	564
"as prepared"	416	530, 525	553
ascorbate-reduced	418	531, 525	554
dithionite-reduced	421, 428	533, 526	556, 561

Spectroscopy. The resonance Raman spectra were recorded at 20 ± 1 °C using a Jobin-Yvon spectrometer (HG2S−UV) and excited with the 406.7- and 413.1-nm lines of a Kr^+ laser (Coherent Innova) and the 441.6-nm line of a He/Cd laser (Liconix). Radiant powers of 5−20 mW were used. The RR spectra shown are the results of unsmoothed sums of 3 to 12 scans. The RR spectra were analyzed with Spectra Calc or Grams/32 software (Galactic Industries). To ascertain the positions of overlapping bands, curve fittings with Lorentzian band shapes and linear backgrounds were made with a nonlinear least-squares program of the Grams/32 software. The frequencies of the weakest RR bands are determined within 1−2 cm^{-1} uncertainties. For the strongest bands, the uncertainty range is decreased to 0.5−1 cm^{-1}.

The ascorbate- and dithionite-reduced bc_1 complexes were prepared anaerobically (*30, 31*). To avoid problems due to the use of potassium ferricyanide under blue/violet excitations (*32*), the hemes of the bc_1 complex were oxidized with ammonium persulfate (*33*). The persulfate- and ferricyanide-oxidized complexes exhibited identical visible electronic spectra. Four oxidation−reduction states of cyt bc_1 were investigated by RR spectroscopy, i.e., the oxidized, "as prepared", ascorbate-reduced and dithionite-reduced forms. Although the laser powers used were low (5−20 mW), heme photoreduction caused by the blue/violet illuminations slightly increases the reduction levels of one (or several) heme(s) of cyt bc_1.

RESULTS

High-Frequency Regions (1300−1650 cm^{-1}) of RR Spectra

The most prominent bands of the high-frequency RR spectra of heme protein corresponded to porphyrin skeletal modes (*18*). With Soret excitations, the ν_4 mode gave rise to the strongest band in the spectra, but large contributions of the ν_2, ν_3, ν_{10}, ν_{11}, ν_{37}, ν_{38}, and ν(CCvinyl) modes were also observed (*23*−*26*). Very similar observations were made in the Soret-excited spectra of cyt bc_1 (Figures 1−5).

ν_4 Regions. The ν_4 regions of RR spectra (1350−1380 cm^{-1}) of oxidized cyt bc_1 were dominated by a band at 1372−1373 cm^{-1} with a bandwidth at half-height (BWHH) of 12 ± 1 cm^{-1} (spectra a in Figure 1A, B, C). A shoulder at 1360−1363 cm^{-1} (BWHH = 12−13 cm^{-1}) represents a small contribution from reduced heme(s) generated by the laser illumination. The RR spectra of the "as prepared" complex indicate a significant heme reduction, because two ν_4 bands of variable relative intensity with the excitation were observed at 1361−1363 and 1372−1374 cm^{-1} (Figure 1, spectra b). The spectra of the ascorbate-reduced form contained major features arising from reduced heme species because the Soret excitations enhance a strong ν_4 mode at 1359−1363 cm^{-1} (BWHH = 11−12 cm^{-1}) with a minor

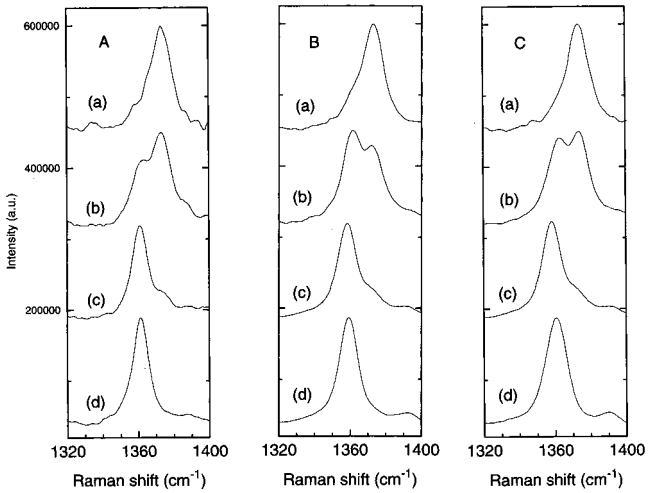

FIGURE 1: The 1300−1400 cm^{-1} regions of RR spectra of the *R. rubrum* cytochrome bc_1 complex excited at 441.6 (A), 413.1 (B), and 406.7 (C) nm. In each panel, spectra a = oxidized complex, spectra b = "as prepared" complex, spectra c = ascorbate-reduced complex, and spectra d = dithionite-reduced complex.

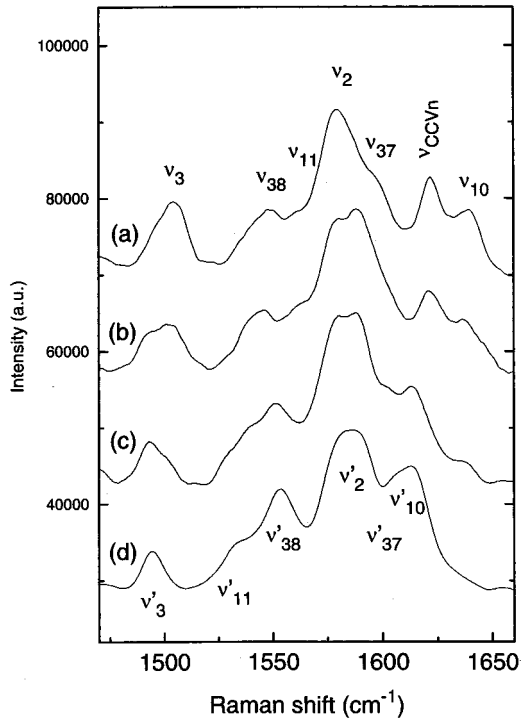

FIGURE 2: The 1470−1660 cm^{-1} regions of RR spectra of the *R. rubrum* cytochrome bc_1 complex at 413.1 nm. (a) oxidized complex; (b) "as prepared" complex; (c) ascorbate-reduced complex; and (d) dithionite-reduced complex. ν_x and ν'_x correspond to assignments for oxidized and reduced heme species, respectively.

component at 1372−1374 cm^{-1} (BWHH = 12 cm^{-1}) (Figure 1, spectra c). The ν_4 band of the dithionite-reduced bc_1 complex was observed at 1361, 1359, and 1360 cm^{-1} with the excitations at 441.6, 413.1, and 406.7 nm, respectively (Figure 1, spectra d). Besides this small frequency shift, a most significant spectral difference concerned the ν_4 bandwidth that is broader with 406.7-nm excitation (BWHH = 15 ± 1 cm^{-1}) than with 413.1- and 441.6-nm excitations (13 ± 1 and 11 ± 1 cm^{-1}, respectively).

ν_3 Regions. With the three Soret excitations used, the ν_3 mode of oxidized cyt bc_1 was seen at 1503−1505 cm^{-1} (Figure 2, and spectra not shown). In the spectra of the "as

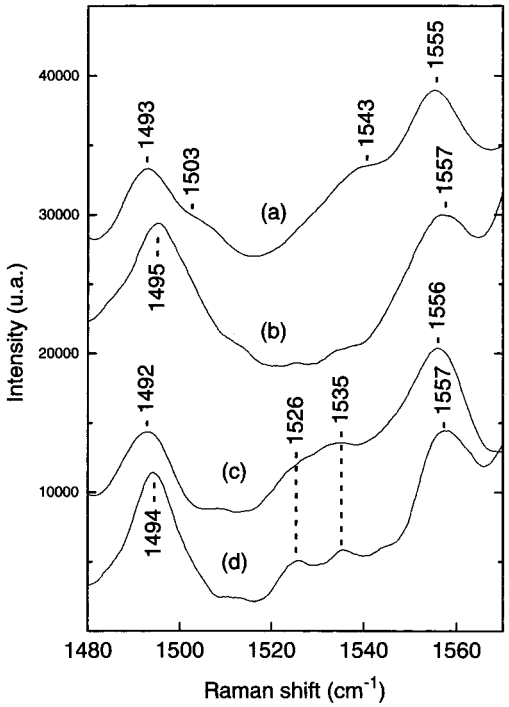

FIGURE 3: the 1480−1570 cm^{-1} regions of RR spectra of the *R. rubrum* cytochrome bc_1 complex. (a, and b) ascorbate-reduced complex excited at 406.7 and 441.6 nm, respectively, (c, and d) dithionite-reduced complex excited at 406.7 and 441.6 nm, respectively.

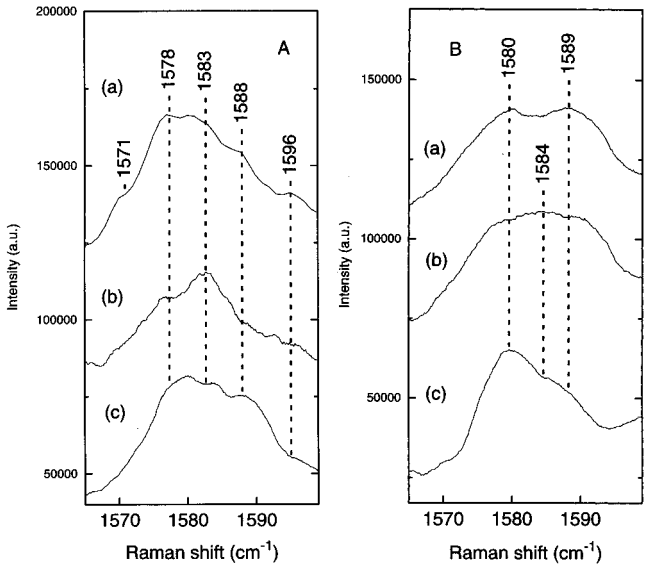

FIGURE 4: The 1560−1600 cm^{-1} regions of RR spectra of the *R. rubrum* cytochrome bc_1 complex. (A) Oxidized complex, excited at (a) 413.1 and (b) 406.7 nm; (c) "As prepared" complex, excited at 406.7 nm. (B) Ascorbate-reduced (a) and dithionite-reduced (b) complex, excited at 413.1 nm; (c) Dithionite-reduced complex, excited at 441.6 nm.

prepared" and ascorbate-reduced forms, this mode had two contributions (Figure 2, spectra b and c, and spectra not shown) confirming the simultaneous presence of oxidized and reduced heme species. The reduced and oxidized hemes showed ν_3 at 1493−1495 and 1502−1504 cm^{-1}, respectively (Figures 2 and 3). The ν_3 mode of the dithionite-reduced cyt bc_1 exhibited clear frequency dispersions (1491−1495 cm^{-1}) and changes in width with the excitation (11−14 cm^{-1}) (Figures 2 and 3).

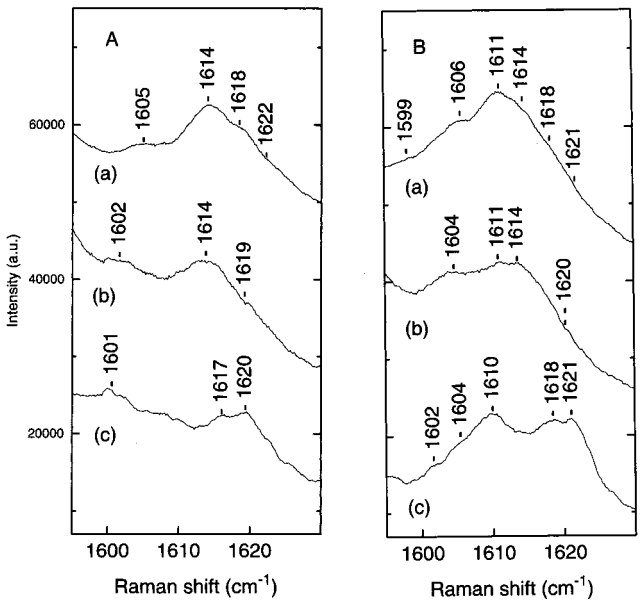

FIGURE 5: The 1600−1630 cm^{-1} regions of RR spectra of the *R. rubrum* cytochrome bc_1 complex. (A) ascorbate-reduced complex excited at 406.7 (a), 413.1 (b), and 441.6 nm (c). (B) dithionite-reduced complex, excited at 406.7 (a), 413.1 (b), and 441.6 nm (c).

ν_{11} *Regions*. The ν_{11} modes of oxidized heme species corresponded to bands in great part hidden by the ν_2 and ν_{38} modes (Figure 2, spectrum a). However, the large downshift of this mode for the reduced hemes allowed the distinction of several components. The "as prepared" form exhibited a component at 1543−1545 cm^{-1} (Figure 2, spectrum b, and spectra not shown). The 1520−1550 cm^{-1} regions of RR spectra of the ascorbate-reduced form, excited at 413.1 nm, showed two ν_{11} bands at 1535−1537 and 1543−1544 cm^{-1} (Figure 2). With the 406.7-nm excitation, the latter component was mainly observed (Figure 3, spectrum a). The RR spectra of the dithionite-reduced complex, excited at 406.7, 413.1, and 441.6 nm, enhanced three ν_{11} bands at 1526−1527, 1535−1536, and 1543−1544 cm^{-1}, the latter component having the smallest contributions (Figures 2 and 3).

ν_2 *Regions*. The ν_2 regions of RR spectra of oxidized cyt bc_1, excited at 441.6 and 413.1 nm, showed a main band at 1578−1579 cm^{-1} (Figure 4A, spectrum a, and spectra not shown). Another ν_2 component at 1583 cm^{-1} dominated the RR spectra excited at 406.7 nm but also contributed in the spectra excited at 413.1 nm (Figure 4A, spectra a and b). A ν_2 shoulder at 1588 cm^{-1} was observable with the 413.1-nm excitation (Figure 4A). When the RR spectra of the oxidized and "as prepared" forms, excited at either 406.7 or 413.1 nm, were compared, the ν_2 regions showed a 1588 cm^{-1} band increasing in relative intensity upon heme c_1 reduction (Figure 4A). The RR spectra of the ascorbate-reduced complex, excited at 413.1 nm, were dominated by two bands at 1580 and 1589 cm^{-1} (Figure 4B, spectrum a). The spectra excited at 406.7 nm exhibited three bands of nearly equal intensity at 1581, 1584, and 1588 cm^{-1} (spectra not shown). The RR spectra of the fully reduced bc_1 complex, excited at 413.1 nm, also contained three bands at 1580, 1584, and 1589 cm^{-1} (Figure 4B, spectrum b). When the RR spectra of the ascorbate- and dithionite-reduced forms, excited at 413.1 nm, were compared, the 1584 cm^{-1} band increased its relative intensity for the fully reduced form (Figure 4B, spectra a and b). The 441.6-nm excitation largely enhanced the ν_2 component at 1580 cm^{-1}, but a minor contribution of the 1584 cm^{-1} component was seen (Figure 4B, spectrum c).

ν_{10} *Regions*. The ν_{10} regions of RR spectra of oxidized cyt bc_1 (1630−1640 cm^{-1}) contained a broad feature in which one can distinguish two overlapping bands at 1635−1636 and 1639−1640 cm^{-1} (Figure 2, spectrum a, and spectra not shown). In the spectra of the "as prepared" and ascorbate-reduced complexes, the corresponding ν_{10} modes exhibited one or two weak bands peaking between 1636 and 1641 cm^{-1} (Table 2).

Taking the intensity of the ν_2 modes as an internal standard, the ν_{10} modes of the reduced hemes were more intense than those of the oxidized hemes (Figure 2). In the spectra of the "as prepared" complex, a single ν_{10} mode was observed at 1618 cm^{-1} (Figure 2). The ν_{10} regions of RR spectra of the ascorbate-reduced form displayed two bands at 1614 and 1617−1618 cm^{-1} (Figure 5A). The former component was observed using the excitations at 413.1 and 406.7 nm (Figure 5A, spectra a and b). The comparison of RR spectra of the dithionite- and ascorbate-reduced forms revealed the enhancement of a new ν_{10} band at 1610−1611 cm^{-1} for the fully reduced form (Figure 5A,B).

ν(CCvinyl) Mode. In the spectra of the oxidized and "as prepared" cyt bc_1 complex, a vinyl stretching vibration [$\nu(CC_{Vn})$] of the b-type hemes was detected as a strong band at 1620−1621 cm^{-1} (Figure 2, spectra a and b). The relative intensity of this mode was decreased when the hemes of cyt bc_1 were gradually reduced (Figures 2 and 5). However, this mode remained located in the 1619−1622 cm^{-1} region (Figure 5 and Table 2).

Mid-Frequency Regions (600−1300 cm^{-1}) of RR Spectra

Peripheral modes of the b- and c-type hemes were characterized in the mid-frequency RR spectra (*23*, *24*). $\nu(C_bC_{substituent})$ (ν_5 and ν_{14}), $\delta(C_mH)$ (ν_{13} and ν_{42}), and $\nu(CS_{thioether})$ modes exhibited significant RR activities when the cyt were Soret-excited (*23*−*26*).

A broad ν_{14} band at 1126 cm^{-1} was the main feature in the 800−1200 cm^{-1} regions of the RR spectra of oxidized cyt bc_1 (Figure 6A, spectrum a). When the reduction state of the bc_1 complex increased, the number of RR bands detected in this region and the signal-to-noise ratios of these bands increased (Figure 6B). This effect permitted the detection of different components for the same mode because the different excitations showed apparent band shift, band broadening, and/or band splitting for the ν_5 (1116−1120 cm^{-1}), ν_{14} (1127−1133 cm^{-1}), ν_{13} (1222−1226 cm^{-1}), and ν_{42} (1205−1216 cm^{-1}) modes (Figure 6). A RR band located in the 1165−1176 cm^{-1} regions and corresponding to the ν_{30} porphyrin mode was also split (Figure 6A,B).

In the 650−700 cm^{-1} regions of RR spectra of the different redox forms of cyt bc_1, the ν_7 mode of b-type hemes and the $\nu(CS_{thioether})$ mode of heme c_1 had large contributions (spectra not shown). These modes are detected, respectively, at 677 and 692 cm^{-1} for the oxidized hemes and at 675 and 689 cm^{-1} for the reduced hemes (spectra not shown, Tables 2 and 3). The $\nu(CS)$ mode of oxidized or reduced heme c_1 was the most active in the RR spectra excited at 406.7 nm, its relative contribution gradually decreasing as the excitation

Table 2: Frequency Ranges (cm^{-1}) and Polarizations (ρ) of the Heme Skeletal Modes Observed in the RR Spectra of the Oxidized, "As Prepared", Ascorbate-Reduced and Dithionite-Reduced *R. rubrum* Cyt bc_1 Complex, Excited at 441.6, 413.1, and 406.7 nm[a]

frequency (ρ)	mode assignment	frequency (ρ)	mode assignment	frequency (ρ)	mode assignment
1639−1641 (dp) 1635−1639 (dp)	ν_{10} (b+c_1)	1500−1505 (p) 1491−1495 (p)	ν_3 (b+c_1) ν'_3 (b+c_1)	717−720 (p) 703−706 (p)	γ'_5 (b+c_1) ν'_7 (c_1)
1617−1618 (dp)	ν'_{10} (c_1)	1465−1466 (dp)	ν'_{28} (c_1)	675−678 (p)	ν_7, ν'_7 (b)
1614 (dp)	ν'_{10} (b_H)	1457−1460 (dp)	ν'_{28} (b)	656−660 (p)	γ'_{20} (c_1)
1610−1611 (dp)	ν'_{10} (b_L)	1400−1402 (dp)	ν_{29} (c_1)	649−654 (p)	γ'_{20} (c_1)
1595−1596 (p)	ν_{37} (c_1)	1389−1394 (dp)	ν'_{29} (b+c_1)	629−633 (p)	ν'_{48} (c_1)
1602−1603 (p)	ν_{37} (b)	1371−1374 (p)	ν_4 (b+c_1)	444−449 (p)	γ'_{22} (c_1)
1604−1606 (p)	ν'_{37} (b+c_1)	1359−1363 (p)	ν'_4 (b+c_1)	361 (p)	ν_{50} (c_1)
1587−1590 (p)	ν_2, ν'_2 (c_1)	1176 (dp)	ν'_{30} (b_L)	355−356 (p)	ν'_{50} (c_1)
1582−1585 (p)	ν_2, ν'_2 (b_H)	1172−1174 (dp)	ν_{30}, ν'_{30} (c_1)	351−353 (p)	ν_8, ν'_8 (b_L)
1578−1581 (p)	ν_2, ν'_2 (b_L)	1165−1167 (dp)	ν_{30}, ν'_{30} (b_H)	346−349 (p)	ν_8, ν'_8 (c_1)
1571 (dp)	ν_{11} (c_1)	1143−1144 (p)	ν'_{43} (c_1)	344−345 (p)	ν_8, ν'_8 (b_H)
1553−1558 (p)	ν'_{38} (b+c_1)	934−938 (dp)	ν'_{32} (b+c_1)	334−337 (p)	γ_6, γ'_6 (b)
1543−1544 (dp)	ν'_{11} (c_1)	919−922 (dp)	ν'_{46} (c_1)	312−316 (p)	ν'_{51} (c_1)
1535−1537 (dp)	ν'_{11} (b_H)	790−793 (p)	ν'_6 (c_1)	297−303 (p)	ν'_{51} (b)
1526−1527 (dp)	ν'_{11} (b_L)	748−752 (dp)	ν'_{15} (b+c_1)	250−253 (p)	γ'_{23} (b)

[a] ν_x, γ_x and ν'_x, γ_x correspond to assignments for oxidized and reduced heme species, respectively.

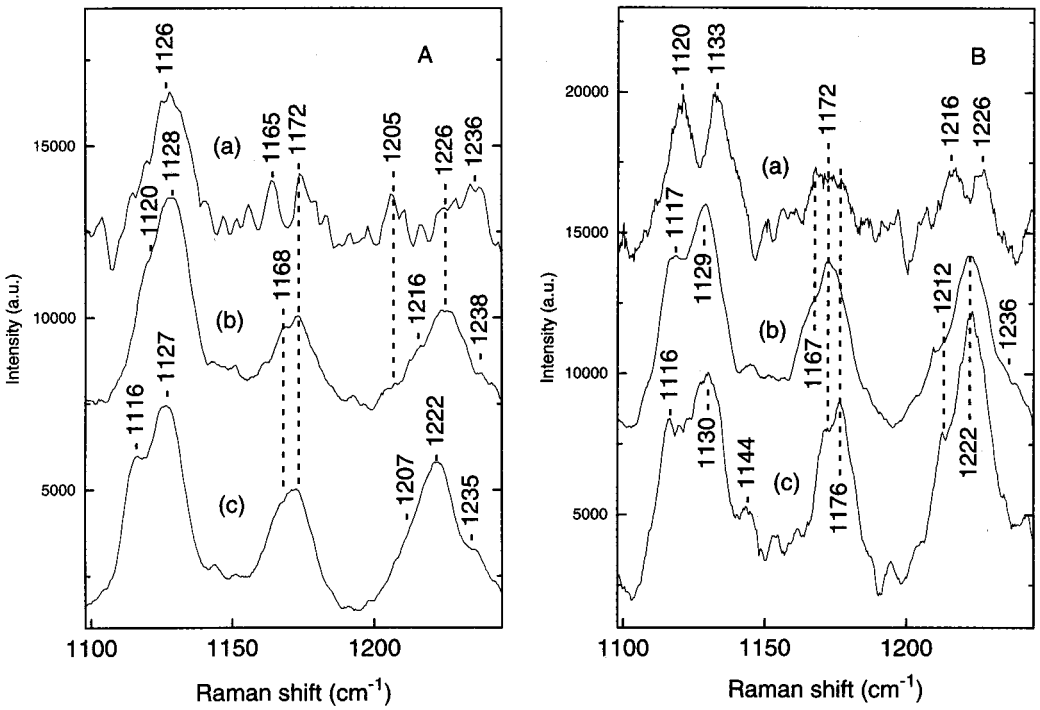

FIGURE 6: The 1100−1250 cm^{-1} regions of RR spectra of the *R. rubrum* cytochrome bc_1 complex. (A) Oxidized (a), "as prepared" (b), and ascorbate-reduced (c) complex, excited at 413.1 nm. (B) Dithionite-reduced complex excited at 441.6 (a), 413.1 (b), and 406.7 (c) nm.

was red-shifted to 413.1 and 441.6 nm (spectra not shown). With the 441.6-nm excitation, the ν_7 mode of the b-type hemes became the major band in the 650−700 cm^{-1} regions.

Low-Frequency Regions (150−600 cm^{-1}) of RR Spectra

Low-frequency modes were previously observed upon B-band excitations of various cyt (*23*−*26*). The principal bands represented deformation modes of either the porphyrin or its peripheral groups (*23, 24*).

Four typical low-frequency RR spectra of cyt bc_1 are shown in Figure 7. In the 180−320 cm^{-1} regions of the spectra of the ascorbate- and dithionite-reduced complexes, excited at 441.6 nm, the most interesting features concern strong specific bands observed at 253 and 250 cm^{-1} (Figure 7, spectra c and d).

The 340−360 cm^{-1} regions of RR spectra of the Soret-excited b- and c-type cyt contained the most intense band (ν_8) (*23*−*26*). Figure 7 shows that this band is broad and asymmetric in the spectra of cyt bc_1. In fact, a blowup of the ν_8 regions shows three components of variable relative intensity with the excitations (Figure 8A,B). The spectra of oxidized cyt bc_1 excited at 441.6 nm exhibited a weak component at 353 cm^{-1} (spectra not shown). The best signal-to-noise ratio of the 413.1-nm excited spectra allowed the deconvolution of four bands at 344, 349, 353 and 361 cm^{-1}. In these spectra, the 353 cm^{-1} component dominated (Figure 8A, spectrum a). Similar features with different relative intensities were detected with the 406.7-nm excitation (Figure 8A, spectrum b). In particular, the contribution of the 353 cm^{-1} component was decreased. The weak 361 cm^{-1} band could be assigned to the ν_{50} mode of ferric cyt c_1 (*26, 31*) (Figure 8A, spectra b and c; Table 2). The spectra of the "as prepared" form were consistent with an overlap of five bands in the 330−370 cm^{-1} regions (Figure 8A, spectrum c). The

Table 3: Frequency Ranges (cm^{-1}) and Polarizations (ρ) of the Peripheral Heme Modes Observed in the RR Spectra of the Oxidized, "As Prepared", Ascorbate-Reduced and Dithionite-Reduced *R. rubrum* Cyt bc_1 Complex, Excited at 441.6, 413.1, and 406.7 nm[a]

frequency (ρ)	mode assignment	frequency (ρ)	mode assignment	frequency (ρ)	mode assignment
1619−1621 (p)	ν_{CCVn}, ν'_{CCVn} (b)	1205 (p)	ν_{42} (c_1)	405−407 (p)	δ'_{CCS} (c_1)
1429−1433 (p)	δ'_{CH2Vn} (b)	1126−1128 (dp)	ν_{14} (b+c_1)	401−402 (p)	$\delta'_{CCaCb2,4}$ (c_1)
1333−1341 (p)	δ'_{CH2Vn} (b)	1129−1133 (dp)	ν'_{14} (b+c_1)	396−397 (p)	δ_{CCS} (c_1)
1315−1317 (p)	$\delta_{CH2,4}$, $\delta'_{CH2,4}$ (c_1)	1116−1122 (p)	ν'_5 (b+c_1)	393−396 (p)	δ'_{CCS} (c_1)
1308−1312 (p)	δ'_{CHVn} (b)	1090−1092 (p)	δ'_{CCH3} (c_1)	390−392 (p)	δ'_{CPr} (c_1)
1298−1301 (p)	$\delta_{CH2,4}$, $\delta'_{CH2,4}$ (c_1)	1001−1004 (p)	ν_{CVn}, ν'_{CVn} (b)	379−381 (p)	δ'_{CPr} (c_1)
1235−1238 (dp)	ν_{13}, ν'_{13} (c_1)	993−995 (p)	ν'_{45} (b)	376−377 (p)	δ_{CPr}, δ'_{CPr} (b)
1226−1227 (dp)	ν_{13}, ν'_{13} (b)	969−976 (p)	ν_{CPr}, ν'_{CPr} (b+c_1)	280−284 (p)	ν_9, ν'_9 (b+c_1)
1222−1224 (dp)	ν'_{13} (b)	689−692 (p)	ν_{CS}, ν'_{CS} (c_1)	268−272 (p) }	ν'_9 (b)
1216 (p)	ν'_{42} (c_1)	420 (p)	$\delta'_{CCaCb2,4}$ (c_1)	261−264 (p) }	
1211−1213 (p)	ν'_{42} (b_L)	416−419 (p)	δ_{CCVn}, δ'_{CCVn} (b_H)	188−190 (p)	ν'_{34} (c_1)
1207 (p)	ν'_{42} (b_H)	409−410 (p)	δ_{CCVn}, δ'_{CCVn} (b_L)		

[a] ν_x, δ_x and ν'_x, δ'_x correspond to assignments for oxidized and reduced heme species, respectively.

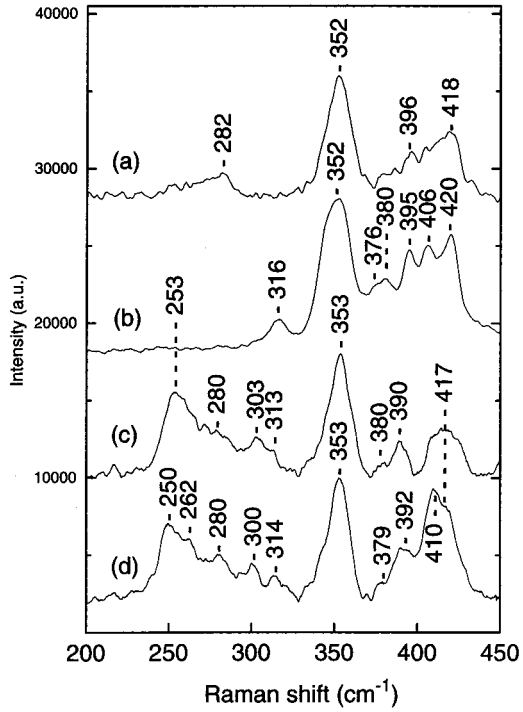

FIGURE 7: Low-frequency regions (200−450 cm^{-1}) of RR spectra of the *R. rubrum* cytochrome bc_1 complex. Oxidized (a) and ascorbate-reduced (b) complexes, excited at 413.1 nm, and ascorbate-reduced (c) and dithionite-reduced (d) complexes, excited at 441.6 nm.

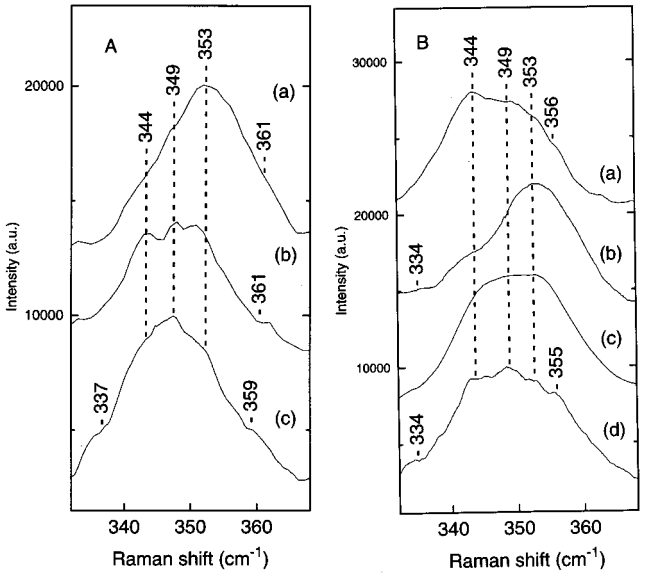

FIGURE 8: The 330−370 cm^{-1} regions of RR spectra of the *R. rubrum* cytochrome bc_1 complex. (A) Oxidized complex, excited at (a) 413.1 and (b) 406.7 nm; (c) "As prepared" complex excited at 406.7 nm. (B) (a) Ascorbate-reduced complex excited at 406.7 nm; Dithionite-reduced complex, excited at (b) 441.6, (c) 413.1, and (d) 406.7 nm.

three central bands at 344, 348, and 353 cm^{-1} were again assignable to ν_8 components. When the spectra of the oxidized and "as prepared" complexes, excited at 406.7 nm, were compared, a relative increase of the 349 cm^{-1} band was observed (Figure 8A, spectra b and c). The RR spectra of the ascorbate-reduced bc_1 complex also exhibited three ν_8 modes peaking at 353, 349, and 344 cm^{-1} (Figure 8B, spectrum a). The high-frequency component was essentially observable with the 441.6-nm excitation (spectra not shown). The relative contribution of the 349 cm^{-1} band was optimized with 413.1-nm excitation but remained visible with 406.7-nm excitation. The 344 cm^{-1} band was seen with the 406.7-nm excitation (Figure 8B, spectrum a). With this latter excitation, an additional shoulder at 356 cm^{-1} was assignable to the ν_{50} mode of ferrous cyt c_1 (*26*, *31*) (Figure 8B, spectrum a; Table 2). As in the RR spectra of the ascorbate-reduced form, those of the dithionite-reduced form exhibited three ν_8 components at 353, 349, and 344 cm^{-1} (Figure 8B, spectra b, c, and d). The comparison of the RR spectra of the ascorbate- and dithionite-reduced complex, excited at 406.7 nm, showed that the relative contribution of the 344 cm^{-1} component was decreased in increasing the reduction state of the b-type hemes (Figure 8B, spectra a and d). The 353 cm^{-1} component of fully reduced cyt bc_1 was the best RR-enhanced ν_8 mode by the 441.6-nm excitation (Figure 8B, spectrum b).

The 370−420 cm^{-1} regions of RR spectra of b- and c-type cyt contained deformation modes of the peripheral heme substituents (*23*−*26*). The spectra of the ascorbate- and dithionite-reduced forms, excited at 413.1 nm, were very similar both in band intensity and band frequency (Figure 7 and spectra not shown). This suggested that the bands observed with the 413.1-nm excitation essentially corresponded to modes of reduced cyt c_1. On the contrary, the RR spectra excited at 441.6 nm exhibited features strongly ressembling those observed for ferroheme b complexes (*37*) (Figure 7). When the 370−420 cm^{-1} regions of RR spectra of the ascorbate- and dithionite-reduced forms, excited at

441.6 nm, were compared, a rising of a band at 410 cm^{-1} was seen (Figure 7).

DISCUSSION

Redox Titration and Absorption Properties of the Hemes of Cytochrome bc_1 Complex

The redox potentials of hemes c_1, b_H, and b_L of the *R. rubrum* bc_1 complex at pH 7.4 are 280, 20, and −85 mV, respectively (*28*). The absorption spectra of persulfate- and dithionite-treated cyt bc_1 show that the three hemes of the complex are oxidized and reduced, respectively (Table 1). Those of the "as prepared" complex indicate that cyt c_1 is predominantly reduced, whereas the diheme cyt b is fully oxidized (Table 1). Given the Nernst equation and the redox potentials of ascorbate (45 mV), cyt c_1 (280 mV), and cyt b_H (20 mV) at pH 7.4, the ascorbate-reduced form is expected to contain a fully reduced heme c_1 and up to 28% of reduced heme b_H.

The absorption spectrum of heme b is markedly red-shifted compared with that of heme c, with the same oxidation and ligation states. For monoheme cyt, however, the amplitudes of the shift differ by ca. 3 and 6 nm for the ferric and ferrous states, respectively (*34*−*36*). For oxidized cyt bc_1 and its isolated cyt c_1, the apparent Soret maximum shifts from 414 to 410 nm, confirming expected small differences for the individual Soret positions of ferrihemes c_1, b_H, and b_L (Table 1). More important differences concern the reduced hemes, because the Soret band of isolated ferrocyt c_1 peaks at 417 nm, whereas that of reduced cyt bc_1 exhibits a main band at 428 nm with a shoulder at 421 nm (Table 1). Moreover, the Soret position of heme b_L is expected to be red-shifted relative to that of heme b_H because of the most electronegative character of its His ligands (*22*, *37*). Thus, the ferrohemes c_1, b_H, and b_L in cyt bc_1 are expected to have a gradually red-shifted B-band. As in monoheme systems (*34*−*36*), the iron reduction of b- and c-type hemes of cyt bc_1 produces a large increase in the molar absorption of the Soret bands.

Activity of the RR Modes of the b- and c-Type Hemes in the B-band Excited Spectra

With Soret excitations, all the intense RR bands of heme complexes are either polarized or depolarized and correspond to modes involving the porphyrin skeleton and/or the heme substituents (*18*, *23*−*26*). The nontotally symmetric heme modes do not contribute as major bands in the RR spectra even excited in the vicinity of the Soret bands (*18*, *23*−*26*, *37*, *38*). In the RR spectra of cyt bc_1, three hemes with two possible oxidation states were investigated. The positions and shapes of the Soret bands do not permit a very selective resonance on each heme type (*21*). However, different B_{00} and/or B_{01} scattering mechanisms are expected to influence the relative intensities of the Raman bands of the oxidized and reduced heme species of cyt bc_1 (*39*−*45*). To extract and discriminate most of the available vibrational information, we used laser excitations with sufficient separations but located within the Soret envelopes of cyt bc_1 (406.7, 413.1, and 441.6 nm). Moreover, previous investigations on b- and c-type hemes allowed the observation of general properties in the Soret enhancement of the main RR bands (*25*, *26*, *31*, *37*, *44*, *45*). The 441.6-nm excitation generally contributed to a better RR scattering of the vibrational modes of the b-type hemes than those of the c-type heme. Inversely, the 406.7-nm excitation relatively enhances the RR contributions of the c-type heme. Based on the high absorbance of the reduced hemes and the laser excitations used, the high RR quantum yield of reduced heme b or c over that of the corresponding oxidized heme constitutes another type of differential enhancement (*25*, *31*, *37*, *44*, *45*). The RR spectra of cyt bc_1 contain much spectral information (Tables 2 and 3). However, we focused our discussion on several of the totally symmetric modes for which both the assignments and sensitivities are well established.

Heme Structures in Cytochrome bc_1 Complex

The RR spectra of cyt bc_1 show band broadening and/or apparent bandshifts for a large number of heme modes (Table 2). Moreover, three components have been characterized for ν_2, ν_8, and ν_{10} (Table 2). Because the frequencies of the latter modes were found sensitive to the porphyrin conformation (*26*, *30*, *31*, *46*, *47*), one can conclude that the three hemes of cyt bc_1 have different structures.

ν_2 Mode. Because of its sensitivity to the heme substituents, the ν_2 frequency is systematically higher for c-type hemes than for b-type hemes, with the same oxidation and ligation states (*25*, *26*, *30*, *31*, *37*, *48*−*53*). The ν_2 mode of six-coordinated low-spin ferroheme b and c compounds is mostly RR-active using preresonant and resonant conditions on the Soret band and, thus, is enhanced by the B_{00} transition (*30*, *37*).

The RR spectra of ferric cyt bc_1 exhibit three ν_2 modes at 1578−1579, 1582−1583, and 1587 cm^{-1}. Those of the fully reduced complex also contain three ν_2 components at 1579−1580, 1584, and 1588−1589 cm^{-1} (Table 2). In the two series of ν_2 components, the highest frequency (1587−1589 cm^{-1}) is assignable to heme c_1. Its relative enhancement with the 413.1-nm excitation for the two oxidation states is due to the fact that this wavelength is between the Soret maxima of ferric and ferrous cyt c_1 (410 and 417 nm, respectively). Moreover, this ν_2 frequency range is within that previously determined for isolated cyt c_1 (*53*). The ν_2 modes of the b-type hemes of cyt bc_1 are assigned to the two remaining bands at 1579 (± 1) and 1583 (± 1) cm^{-1}. The 1578 cm^{-1} component of ferric cyt bc_1 is relatively enhanced at 413.1 nm, a wavelength close to the Soret maxima of ferrihemes b (Table 1). The 1580 cm^{-1} component of reduced cyt bc_1 is enhanced with the 441.6-nm excitation and appears to be in resonance with the b-type ferrous heme with a red-shifted Soret absorption, likely heme b_L. The activity of the 1583 (± 1) cm^{-1} band is consistent with a heme b_H assignment.

ν_8 Mode. This low-frequency mode was assigned to a coupled vibration involving Fe−N(pyrrole) stretch and C_b-(pyrrole)-substituent deformation (*23*, *24*). In the spectra of metalloporphyrins and monoheme proteins, ν_8 is isolated from other neighboring strong bands and is RR-enhanced by the B_{00} transition (*25*, *39*−*41*, *44*). The sensitivity of the ν_8 frequency to the 2,4-substituents appears unsignificant because its frequency range is practically the same for b- and c-type cyt, i.e., 344−349 and 343−350 cm^{-1}, respectively (*25*, *26*, *48*−*50*).

The ν_8 regions of the RR spectra of the bc_1 complex contain three strong bands with relative intensities depending

on the excitation. For all the redox forms, three components are observed at 344, 348−349, and 351−353 cm^{-1} (Table 2). On the basis of the B_{00} activation of ν_8, the 348−349 cm^{-1} band, enhanced by the 406.7-nm excitation, is in one hand associated with heme c_1. On the other hand, the behavior of the 353 cm^{-1} component follows that of the ν_2 component assigned to heme b_L (1578−1580 cm^{-1}), i.e., it is enhanced by the 413.1-nm excitation for the oxidized form and by the 441.6-nm excitation for the reduced form. This ν_8 component is thus assigned to heme b_L. Finally, the remaining ν_8 component at 344−345 cm^{-1} is assigned to heme b_H.

There is no established relationship between the porphyrin structure and the ν_8 frequency (*46*). However, a major ν(Fe−N(pyrrole)) contribution in ν_8 suggests that its frequency is sensitive to changes in metal-pyrrole bond length following changes in porphyrin conformation. A recent investigation on Ni(II)-porphyrins showed that the ν_2 frequency is decreased from 1578 to 1572 cm^{-1} when the macrocycle structure is changed from planar to ruffled (*47*). The same transconformation increases the ν_8 frequency from 392 to 401 cm^{-1}. Several mitochondrial ferricyt c that stabilize a saddled heme structure have a ν_8 mode at 349−351 cm^{-1} (*23, 38*). For a more planar heme like in ferricyt c_2, the ν_8 frequency is downshifted to 345−346 cm^{-1} (*26, 54*). Therefore, an increased frequency of ν_8 again indicates an increased out-of-plane deformation of the heme macrocycle. The ν_8 component assigned to heme c_1 (348−349 cm^{-1}) is close to the frequency range of the mitochondrial cyt c, indicating similar heme structures for cyt c and c_1.

Ferrous b-type cyt and FePP(ImH)$_2$ complexes have a ν_8 mode at 344−347 cm^{-1}, the iron oxidation slightly upshifting this frequency range to 347−349 cm^{-1} (*25, 37, 48−50*). In model compounds, the iron oxidation induces a shortening of the Fe−N(pyrrole) bonds as well as a change in porphyrin conformation from a nearly planar to a slightly ruffled macrocycle (*55*). The ν_8 component of heme b_H at 344−345 cm^{-1} is therefore assignable to a nearly planar or slightly ruffled structure. On the contrary, the ν_8 frequency corresponding to heme b_L is higher by ca. 8 cm^{-1} (352−353 cm^{-1}) and is attributed to a strongly ruffled porphyrin.

ν_{10} Mode. This asymmetric C_aC_m stretching mode is highly sensitive to out-of-plane porphyrin distortions (*26, 30, 46, 47*) and RR-enhanced by the $B_{0,1}$ transition in the Soret region (*40, 42, 43*). With the B-band excitations used generally, ν_{10} of ferroheme c consequently is relatively weaker than that of ferroheme b (*26, 30, 31, 48−53*).

The ν_{10} mode of the oxidized hemes of cyt bc_1 consists of one or two bands peaking at 1636−1641 cm^{-1}. The redox titrations of the bc_1 complex do not allow the attribution of the ν_{10} components to the different heme species. This difficulty may be explained by the relative weakening of the ν_{10} bands of the oxidized hemes in the RR spectra of the "as prepared" and ascorbate forms and by the conformational flexibilities of the ferrihemes that broaden these bands (*26*).

RR investigations on a mitochondrial ferrous bc_1 complex, excited in the Q-band, characterized two ν_{10} bands at 1612 and 1620 cm^{-1}. However, the heme assignments were not made (*20*). The ν_{10} regions in our RR spectra of a bacterial bc_1 complex support conformational differences for the three reduced hemes. The ν_{10} mode of reduced heme c_1 at 1618 ($\pm$1) cm^{-1} is partly overlapped by a vinyl mode of the b-type hemes at ca. 1621 cm^{-1}. With Q-band excitations, ν_{10} of ferrocyt c_1 was located at 1619 cm^{-1} (*22*). The sequential reduction of cyt bc_1 shows a 1614 cm^{-1} band beginning to be visible in the RR spectra of the ascorbate-reduced form and also discernible in the spectra of the dithionite-reduced form. Recalling that ascorbate partially reduces heme b_H, the 1614 cm^{-1} band is thus assigned to the ν_{10} mode of reduced heme b_H. Finally, a 1610−1611 cm^{-1} band, only observed in the spectra of the fully reduced cyt bc_1, is attributed to the ν_{10} of reduced heme b_L. Because of the activation of ν_{10} by the B_{01} transitions, the heme assignments of the ν_{10} components are easier than those of the ν_2 and ν_8 components enhanced by the B_{00} transitions. In fact, the sequential activity of the ν_{10} modes of ferrous hemes exactly follows the reductive titration of the three hemes of cyt bc_1 [heme c_1 (1618 cm^{-1}), heme b_H (1614 cm^{-1}), and heme b_L (1610 cm^{-1})]. The characterization of these three ν_{10} frequencies points to different structures with small conformational flexibilities for ferrous hemes c_1, b_H, and b_L.

Pyrrole Ring Modes. Significant differences in the frequencies and widths of ν_4 [ν(pyrrole half-ring)$_{sym}$] of the fully reduced cyt bc_1 complex were measured. Among other modes involving pyrrole ring stretch (*23, 24*), we noticed that ν_{30} exhibits a band splitting (Table 2). These observations constitute additional probes for structural differences of hemes c_1, b_H, and b_L in ferrous cyt bc_1.

ν_{11} Mode. This $\nu(C_bC_b)$ mode is strongly influenced by the electronic interactions of the Fe(II)-ligands (*18, 30, 31, 37*). Three ν_{11} bands at 1527, 1534, and 1539 cm^{-1} were identified in the Q-band excited spectra of a mitochondrial ferrous bc_1 complex (*20*). In the Q-band excited spectra of *Rhodobacter capsulatus* cyt bc_1, homologous bands at 1528, 1536 and 1543 cm^{-1} were assigned, respectively, to the ν_{11} mode of ferrous hemes b_L, b_H, and c_1 (*22*). The ν_{11} mode of the same hemes in the fully reduced bc_1 complex from *R. rubrum*, excited in the B-band, is observed at 1526−1527, 1535−1537 and 1543−1544 cm^{-1}, respectively (Table 2). The 7−10 cm^{-1} shift in the ν_{11} frequency of hemes b_H and b_L of mitochondrial and bacterial bc_1 complexes can therefore be attributed to a conserved difference in electronegativity of the histidylimidazole ligands (*22, 37*). The Fe(II)PP(ImH)$_2$ and Fe(II)PP(Im$^-$)$_2$ complexes, prepared in detergent solution, were previously investigated to serve as models for the coordination and environment of the b-type hemes in the bc_1 complex (*37*). The b-type hemes of cyt bc_1 are indeed embedded in a hydrophobic environment and coordinated by His ligands (*1, 7*). The RR spectra of the Fe(II)PP models showed that ν_{11} is downshifted from 1539 to 1517 cm^{-1} upon deprotonation of the two ImH (*37*). Assuming that (i) this 22-cm^{-1} downshift corresponds to the formation of two axial negative charges and (ii) the ν_{11} frequency is linearly correlated with the overall charge of the imidazole ligands (*37*), the ν_{11} frequency of heme b_L (1527 $\pm$ 1 cm^{-1}) is calculated to correspond to a total negative charge of 1.0 ($\pm$ 0.1) on the two histidylimidazole rings.

Conformations of the b-Type Hemes. The asymmetric broadening or the splitting detected for several porphyrin modes of the ferrous cyt bc_1 complex (ν_2, ν_4, ν_8, ν_{10}, ν_{30}) are illustrative of different structures for the tetrapyrrole macrocycle of hemes c_1, b_H, and b_L. From the ν_2 and ν_8 regions of the RR spectra of the oxidized cyt bc_1 complex,

one can conclude that structural differences also concern the ferric state of the three hemes.

The monomeric Fe(II)PP(ImH)$_2$ complex has ν_2, ν_8, and ν_{10} modes at 1584, 345, and 1616 cm^{-1}, respectively. The ligand deprotonations slightly shift these modes to 1583, 346, and 1613 cm^{-1}, respectively (*37*). On the basis of these data, the structure of the ferrous bis(His)-heme b_L grouping appears to be distorted with corresponding modes at 1580, 352, and 1610 cm^{-1} (Table 2). The low ν_{10} frequency may be associated only partly with the electronegative character of the His ligands of heme b_L (*22*, *37*) because a ν_{11} frequency at 1527 cm^{-1} cannot be associated with fully ionized ligands (*37*) (vide supra). Thus, the 1610 cm^{-1} frequency for ν_{10} is mainly attributed to a distorted porphyrin (*26*, *30*, *46*, *47*). Considering that ν_2 and ν_8 are sensitive to the heme conformation and weakly sensitive to the ImH deprotonations (*37*, *47*), the 1580 and 352 cm^{-1} frequencies are also primarily indicative of a marked distortion of heme b_L.

The ν_2, ν_8, and ν_{10} modes of ferroheme b_H are assigned at 1584, 344, and 1614 cm^{-1}, respectively (Table 2). The ν_2 and ν_8 frequencies are close to those of Fe(II)PP(ImH)$_2$ (1584 and 345 cm^{-1}, respectively) (*37*). From the ν_{10} frequency of this model (1616 cm^{-1}), the 2 cm^{-1} shift observed for heme b_H is interpreted in the frame of a small porphyrin deformation (*26*, *30*, *31*).

Among the low-frequency modes, a strong band is observed at 250−253 cm^{-1} in the RR spectra of ascorbate- and dithionite-reduced bc_1 complexes excited at 441.6 nm (Figure 7). Such an enhancement suggests that it originates from the b-type ferrohemes. No homologous band was found in the RR spectra of Fe(II)PP(ImH)$_2$ and Fe(II)PP(Im$^-$)$_2$ (*37*). Moreover, an inspection of the available RR data on ferrous b-type cyt (*25*, *48*−*50*) shows that the 250−253 cm^{-1} band is specific to the diheme cyt b of the bc_1 complex. In the absence of isotopic data, the vibrational origin of this band cannot be established. However, from RR data on Fe(II)PP compounds, the most likely assignment for the 250−253 cm^{-1} band should be a mode involving an out-of-plane pyrrole tilt (γ_{23}) (*18*, *24*). The activation of this E_g mode could be related to a particular out-of-plane heme distortion generated by a near-perpendicular arrangement of the His ligands of hemes b_H and b_L (*13*, *24*, *56*).

Peripheral Interactions between Hemes and Protein in Cytochrome bc_1 Complex

Modes Involving the Thioether Linkages of Heme c_1. The $\nu(CS_{thioether})$ mode is observed at 692 and 689 cm^{-1} when heme c_1 of cyt bc_1 is oxidized and reduced, respectively (Table 3). Deformation modes of the thioether bridges [δ(CCS)] were attributed to a band pair at 394 and 401 cm^{-1} for ferrocyt c (*23*). The bands observed at 395 and 406 cm^{-1} in the RR spectra of the ascorbate- and dithionite-reduced cyt bc_1, excited at 413.1 nm, are associated with these modes of ferroheme c_1. The slight frequency shifts observed for the ν(CS) and δ(CCS) modes of cyt c_1 (689, 395, and 406 cm^{-1} versus 692, 394, and 401 cm^{-1} for cyt c) reflect some subtle differences in the structure of the thioether links and/or in the interactions of these groups with the protein.

Modes Involving the Vinyl Groups of Hemes b. The frequency of the $\nu(CC_{Vn})$ mode of cyt bc_1 (1619−1622 cm^{-1}) is close to that found for FePP(ImH)$_2$ complexes (1623 cm^{-1}) and suggests weak constraints on the C=C vinyl bonds of the b-type hemes (*37*). The frequencies of the C_b(pyrrole)-CC_{Vn} deformation modes are expected to bring more information on the vinyl conformations (*24*). For the FePP(ImH)$_2$ compounds, these mode are attributed to two overlapping bands at 414 and 420 cm^{-1} (*37*). On the one hand, the broad 417 cm^{-1} band observed in the RR spectra of ascorbate-reduced cyt bc_1, excited at 441.6 nm, is assigned to a $\delta(C_bCC_{Vn})$ mode of reduced heme b_H. On the other hand, the RR activation of a 410 cm^{-1} band in the spectra of the fully reduced cyt bc_1, excited at 441.6 nm, can be attributed to an enhancement of a vinyl deformation of ferroheme b_L (Table 3). These assignments suggest different conformations of at least one vinyl group of hemes b_H and b_L. Moreover, the lowest frequency observed for the $\delta(C_bCC_{Vn})$ mode of heme b_L indicates that the protein exerts more constraints at its periphery than for heme b_H.

Methyl and Proton Substituents of Hemes b and c_1. The ν_5 and ν_{14} modes have similar origins [$\nu(C_b$-methyl)] and are observed at 1117−1121 and 1129−1135 cm^{-1}, respectively, for various heme b and heme c complexes (*23*−*26*, *38*, *49*). The RR spectra of cyt bc_1, under different redox states, exhibit inhomogeneous broadening and/or apparent frequency shifts for these modes. The 1126−1128 cm^{-1} band seen for the less reduced states of cyt bc_1 can be associated with ν_{14} of ferroheme c_1. The highest frequencies (1129−1133 cm^{-1}) observed for the most reduced states are associated with the same mode of ferrohemes b (Table 3). This ν_{14} shift as well as the frequency dispersion of ν_5 (1116−1122 cm^{-1}) indicate that the methyl conformations are different for the b- and c-type hemes in cyt bc_1 (Table 3).

Deformation modes of methine protons (ν_{13} and ν_{42}) were assigned in the 1200−1240 cm^{-1} regions of RR spectra (*23*, *24*). With B-band excitations, these modes are enhanced more for ferrohemes than for ferrihemes (*25*, *26*, *38*, *48*). On the one hand, ν_{42} and ν_{13} of ferrous c-type cyt are detected at 1206−1216 and 1229−1232 cm^{-1}, respectively (*23*, *26*, *38*). On the other hand, cyt b_2 and FePP(ImH)$_2$ exhibit ν_{13} at 1225−1232 cm^{-1}, but no ν_{42} mode (*25*, *37*, *49*). Overlapping bands of different relative intensity and apparent frequency are seen in the 1200−1240 cm^{-1} regions of RR spectra of the bc_1 complex (Table 3). Both the strong ν_{13} activation of the ferrohemes and the sequential reduction of cyt bc_1 allow the assignment of the 1226 cm^{-1} band to the ν_{13} mode of reduced heme c_1 (Table 3). Similarly, the intense 1222 cm^{-1} band, arising when the reduction level of cyt bc_1 is increased, is assigned to the ν_{13} mode of ferrohemes b_H and b_L. This low ν_{13} frequency is indicative of some strains at the periphery of the b-type hemes. The bands observed at 1205, 1216, 1207, and 1212 cm^{-1} in the reductive titration of the bc_1 complex (Table 3) are candidates for a ν_{42} assignment of oxidized heme c_1, reduced heme c_1, reduced heme b_H, and reduced heme b_L, respectively, and could be associated with different out-of-plane methine distortions (*23*).

Structures and Interactions of the b-Type Hemes in Cytochrome bc_1 Complex

Our RR data characterized significant differences in the structures of the three hemes of cyt bc_1. Differences in conformation of some peripheral groups were also detected.

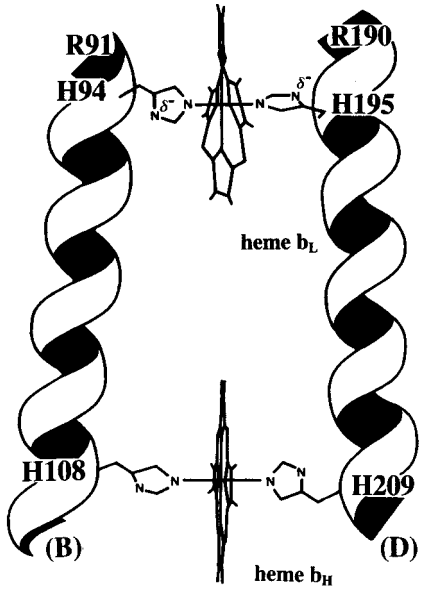

FIGURE 9: Schematic representation of the structures and binding sites of the b-type hemes in the *R. rubrum* cytochrome bc_1 complex.

From all these observations, one can conclude that the cyt bc_1 polypeptides exert different contraints on the hemes to modulate the redox properties.

According to numerous experimental data and molecular modeling, hemes b_H and b_L of all the bc_1 complexes are located between four putative transmembrane helices A, B, C, and D (*1*, *3*, *7*). The recent structure of a mitochondrial cyt bc_1 supports this conclusion because a four-helix bundle made by these helices constitutes the binding domain of b-type hemes (*12*). Helices B and D provide the four heme ligands, i.e., H83/H182 and H97/H196 for heme b_L and heme b_H, respectively. In the amino acid sequences of the bc_1 complexes, 14 amino acid residues separate the first and the second conserved His ligands of each heme [H83(b_L)/H97-(b_H) and H182(b_L)/H196(b_H) for beef heart; H94/H108 and H195/H209 for *R. rubrum*] (*58*) (Figure 9). Four conserved Gly residues on helices A and C appear to play a role in both the structure and the packing of hemes b_H and b_L of the bc_1 complexes (*58*−*60*). In fact, tilts and/or kinks of helices A, B, C and D probably make the heme/protein arrangements different on the positive and negative sides of the cyt b subunit (*12*). Toward the positive side, the sections of helices A, B, C, and D are arranged in a square and very close to heme b_L, whereas the protein environment around heme b_H is both less symmetric and less dense (*12*). The higher degree of porphyrin distortion found for heme b_L as well as the stronger deformation of its axial coordination and of some of peripheral groups are interpreted in the context of stronger constraints exerted by the helices on this heme (Figure 9).

The electronegative character of at least one of the two His ligands of heme b_L may be related to the presence of two conserved Arg residues, located in the amino acid sequences three or five residues before the His ligands of hemes b_L (R80 and R177 for beef heart and R91 and R190 for *R. rubrum*) (*1*, *3*, *7*, *58*) (Figure 9). Actually, a well-oriented guanidium group of an Arg residue can stabilize an anionic heme ligand (*37*).

The different ligand electronegativities as well as the different structures of the porphyrin can explain the differences in midpoint potential of the two b-type hemes of *R. rubrum* cyt bc_1. On the one hand, the most negative potential of heme b_L can be associated largely with a partial negative charge on its His ligands (*37*). On the other hand, changes from planar to nonplanar structures could decrease the midpoint potential of hemes (*61*). However, the amplitudes of redox shifts due to porphyrin distortions remain to determine.

CONCLUSION

Using B-band excitations, the present RR study has characterized several vibrational modes arising from the b- and c-type hemes of the *R. rubrum* cyt bc_1 complex. On the one hand, the frequencies of skeletal heme modes show that the b- and c-type hemes have different macrocycle conformations. On the other hand, the frequency dispersions of peripheral modes are indicative of differences in heme/protein interaction for the three hemes. All these data suggest that heme b_L has a more constrained protein environment than heme b_H. The obtained vibrational information will also serve to further evaluate the effects of cofactor or inhibitor binding and of mutated amino acids on the structures and environments of the cyt bc_1 chromophores.

REFERENCES

1. Trumpower, B. L. (1990) *Microbiol. Rev. 54*, 101−129.
2. Anderson, J. M. (1992) *Photosynth. Res. 34*, 341−357.
3. Gennis, R. B., Barquera, B., Hacker, B., Van Doren, S. R., Arnaud, S., Crofts, A. R., Davidson, E., Gray, K. A., and Daldal, F. (1993) *J. Bioenerg. Biomembr. 25*, 195−209.
4. Yu, C.-A., and Yu, L. (1993) *J. Bioenerg. Biomembr. 25*, 259−273.
5. Vasquez-Acevedo, M., Antaramian, A., Corona, N., and Gonzalez-Halphen, D. (1993) *J. Bioenerg. Biomembr. 25*, 401−410.
6. Cramer, W. A., Martinez, S. E., Huang, D., Tae, G.-S., Everly, R. M., Heymann, J. B., Cheng, R. H., Baker, T. S., and Smith, J. L. (1994) *J. Bioenerg. Biomembr. 26*, 31−47.
7. Brandt, H., and Trumpower, B. (1994) *Crit. Rev. Biochem. Mol. Biol. 29*, 165−197.
8. Mitchell, P. (1976) *J. Theor. Biol. 62*, 327−367.
9. Beattie, D. S. (1993) *J. Bioeng. Biomembr*. 25, 233−244.
10. Knaff, D. B. (1993) *Photosynth. Res. 35*, 117−133.
11. Schägger, H., Link, T. A., Engel, W. D., and von Jagow, G. (1986) *Methods Enzymol. 126*, 224−237.
12. Xia, D., Yu, C.-A., Kim, H., Xia, J.-H., Kachurin, A. M., Zhang, L., Yu, L., and Deisenhofer, J. (1997) *Science 277*, 60−66.
13. Salerno, J. C. (1984) *J. Biol. Chem. 259*, 2331−2336.
14. Widger, W. R., Cramer, W. A., Herrmann, R. G., and Trebst, A. (1984) *Proc. Natl. Acad. Sci. U.S.A. 81*, 674−678.
15. Saraste, M. (1984) *FEBS Lett. 166*, 367−372.
16. Crofts, A., Hacker, B., Barquera, B., Yun, C.-H., and Gennis, R. (1992) *Biochim. Biophys. Acta 1101*, 162−165.
17. Ohnishi, T., Schägger, H., Meinhardt, S. W., LoBrutto, R., Link, T. A., and von Jagow, G. (1989) *J. Biol. Chem. 264*, 735−744.
18. Spiro, T. G., and Li, X.-Y. (1988) in *Biological Applications of Raman Spectroscopy* (Spiro, T. G., Ed.) Vol. 3, pp 1−37, J. Wiley & Sons, New York.
19. Kitagawa, T., and Ozaki, Y. (1987) *Struct. Bonding 64*, 71−114.
20. Adar F., and Erecinska, M. (1978) *Biochemistry 17*, 5484−5488.
21. Hobbs, D. D., Kriauciunas, A., Güner, S., Knaff, D. B., and Ondrias, M. R. (1990) *Biochim. Biophys. Acta 1018*, 47−54.
22. Gao, F., Qin, H, Simpson, M. C., Shelnutt, J. A., Knaff, D. B., and Ondrias, M. R. (1996) *Biochemistry 35*, 12812−12819.

23. Hu, S., Morris, I. K., Singh, J. P., Smith, K. M., and Spiro, T. G. (1993) *J. Am. Chem. Soc. 115*, 12446−12458.
24. Hu, S., Smith, K. M., and Spiro, T. G. (1996) *J. Am. Chem. Soc. 118*, 12638−12646.
25. Desbois, A., Tegoni, M., Gervais, M., and Lutz, M. (1989) *Biochemistry 28*, 8011−8022.
26. Othman, S., Fitch, J., Cusanovich, M. A., and Desbois, A. (1997) *Biochemistry 36*, 5499−5508.
27. Andrews, K. M., Crofts, A. R., and Gennis, R. B. (1990) *Biochemistry 29*, 2645−2651.
28. Güner, S., Robertson, D. E., Yu, L., Qiu, Z., Yu, C.-A., and Knaff, D. B. (1991) *Biochim. Biophys. Acta 1058*, 269−279.
29. Kriauciunas, A., Yu, L., Yu, C.-A., Wynn, R. M., and Knaff, D. B. (1989) *Biochim. Biophys. Acta 976*, 70−76.
30. Othman, S., Le Lirzin, A., and Desbois, A. (1994) *Biochemistry 33*, 15437−15448.
31. Othman, S., and Desbois, A. (1998) *Eur. Biophys. J.* (in press).
32. Chottard, G. (1989) *Biochim. Biophys. Acta 997*, 155−157.
33. Böhme, H., Brütsch, S., Weithmann, G., and Böger, P. (1980) *Biochim. Biophys. Acta 590*, 248−260.
34. Meyer, T. E., and, Kamen, M. D. (1982) *Adv. Protein Chem. 35*, 105−212.
35. Strittmatter, P., and Ozols, J. (1966) in *Hemes and Hemoproteins* (Chance, B., Estabrook, R. W., and Yonetani, T., Eds. pp 447−463, Academic Press, New York.
36. Iwatsubo, M., and Risler, J. L. (1969) *Eur. J. Biochem. 9*, 280−285.
37. Desbois, A., and Lutz, M. (1992) *Eur. Biophys. J. 20*, 321−335.
38. Desbois, A. (1994) *Biochimie 76*, 693−707.
39. Shelnutt, J. A., O'Shea, D. C., Yu, N.-T., Cheung, L. D., and Felton, R. H. (1976) *J. Chem. Phys. 64*, 1156−1165.
40. Cheung, L. D., Yu, N.-T., and Felton, R. H. (1978) *Chem. Phys. Lett. 55*, 527−530.
41. Desbois, A., Lutz, M., and Banerjee, R. (1981) *Biochim. Biophys. Acta 671*, 177−183.
42. Shelnutt, J. A., and O'Shea, D. C. (1978) *J. Chem. Phys. 69*, 5361−5374.
43. Shelnutt, J. A. (1981) *J. Chem. Phys. 74*, 6644−6657.
44. Champion, P. M., and Albrecht, A. C. (1979) *J. Chem. Phys. 71*, 1110−1121.
45. Stallard, B. R., Callis, P. R., Champion, P. M., and Albrecht, A. C. (1984) *J. Chem. Phys. 80*, 70−82.
46. Jentzen, W., Simpson, M. C., Hobbs, J. D., Song, X., Ema, T., Nelson, N. Y., Medforth, C. J., Smith, K. M., Veyrat, M., Mazzanti, M., Ramasseul, R., Marchon, J.-C., Takeuchi, T., Goddard, W. A., III, and Shelnutt, J. A. (1995) *J. Am. Chem. Soc. 117*, 11085−11097.
47. Jentzen, W., Unger, E., Song, X.-Z., Jia, S.-L., Turoska-Tyrk, I., Scheitzer-Stenner, R., Dreybrodt, W., Scheidt, W. R., and Shelnutt, J. A. (1997) *J. Phys. Chem. A 101*, 5789−5798.
48. Kitagawa, T., Sugiyama, T., and Yamano, T. (1982) *Biochemistry 21*, 1680−1686.
49. Hurst, J. K., Loehr, T. M., Curnutte, J. T., and Rosen, H. (1991) *J. Biol. Chem. 266*, 1627−1634.
50. Escriou, V., Laporte, F., Vignais, P. V., and Desbois, A. (1997) *Eur. J. Biochem. 245*, 505−511.
51. Verma, A. L., Kimura, K., Nakamura, A., Yagi, T., Inokuchi, H., and Kitagawa, T. (1988) *J. Am. Chem. Soc. 110*, 6617−6623.
52. Adar, F. (1978) *J. Phys. Chem. 82*, 230−234.
53. Lou, B.-S., Hobbs, J. D., Chen, Y.-R., Yu, L., Yu, C.-A., and Ondrias, M. R. (1993) *Biochim. Biophys. Acta 1144*, 403−410.
54. Benning, M. M., Wesenberg, G., Caffrey, M. A., Barsch, R. G., Meyer, T. E., Cusanovich, M. A., Rayment I., and Holden, H. M. (1991) *J. Mol. Biol. 220*, 673−685.
55. Scheidt, W. R., and Gouterman, M. (1983) in *Iron Porphyrins I* (Lever, A. B. P., and Gray, H. B., Eds.) pp 89−139, Addison-Wesley, London
56. Robertson, D. E., Ding, H., Chelminski, P. R., Slaughter, C., Hsu, J., Moomaw, C., Tokito, M., Daldal, F., and Dutton, P. L. (1993) *Biochemistry 32*, 1310−1317.
57. Walker, F. A., Huynh, B. H., Scheidt, W. R., and Osvath, S. R. (1986) *J. Am. Chem. Soc. 108*, 5288−5297.
58. Degli Esposti, M., De Vries, S., Crimi, M., Ghelli, A., Patarnello, T., and Meyer, A. (1993) *Biochim. Biophys. Acta 1143*, 243−271.
59. Tron, T., Crimi, M., Colson, A.-M., and Degli Esposti, M. (1991) *Eur. J. Biochem. 199*, 753−760.
60. Saribas, A. S., Ding, H., Dutton, P. L., and Daldal, F. (1997) *Biochim. Biophys. Acta 1319*, 99−108.
61. Barkigia, K. M., Chantranupong, L., Smith, K. M., and Fajer, J. (1988) *J. Am. Chem. Soc.* 110, 7566−7567.

BI9805487